Introducing ink spreading within the cellular Yule-Nielsen modified Neugebauer model

Romain Rossier, Thomas Bugnon, Roger D. Hersch, School of Computer and Communication Sciences, Ecole Polytechnique Fédérale de Lausanne (EPFL), Switzerland

Abstract

We propose an extension of the cellular Yule-Nielsen spectral Neugebauer model accounting for ink spreading of each ink within each subdomain. Characterization of the ink spreading within a given subdomain is performed by fitting the mid-range weights of subdomain node reflectances with the goal of minimizing the sum of square differences between predicted and measured mid-range reflectances. We show that the mid-range weights within a subdomain can be either separately fitted on three halftones or jointly fitted on a single halftone. Accounting for ink spreading considerably improves the prediction accuracy and requires only one additional measurement per subdomain. These additional measurements do not necessarily require spectral measurements. Instead, ink spreading can also be characterized with red, green and blue sensor responses without decreasing the model reflectance prediction accuracy.

Introduction

A printer is characterized by the relationship between the printer's input in terms of nominal surface coverages of the inks and the resulting output color. This relationship is often obtained by printing hundreds of color halftones at different combinations of ink surface coverages. Another approach consists in modeling the interaction of the light and the print according to a spectral prediction model [1] [2] such as the Yule-Nielsen modified spectral Neugebauer model (YNSN). The colorants contributing to the halftone reflectance, also called Neugebauer primaries, are formed by the paper white, the inks and their superpositions. The predicted spectral reflectance of color halftones at given ink surface coverages is obtained by the sum of the colorant spectral reflectances weighted by their corresponding area coverages, where a scalar exponent (*n*-value) is used to model the non linear relationship between the colorant spectral reflectances and the resulting halftone reflectance. Thanks to a spectral prediction model, the printer can be characterized with a small number of measurements.

In order to provide a higher prediction accuracy, Heuberger et al. [3] proposed the Cellular Neugebauer model. Subdomains are created by dividing the CMY surface coverage unit cube into 8 subcubes, called subdomains, formed by combinations of 0%, 50% and 100% surface coverages of the cyan, magenta and yellow inks. With such a subdivision, the number of primary reflectances increases from 8 to 27. Each subdomain, for example the one formed by ink coverages varying between 0% and 50%, forms itself a spectral Neugebauer model formed by 8 of the 27 primary reflectances. Balasubramanian [4] has shown that the cellular subdivision is also applicable to the Yule-Nielsen spectral Neugebauer model (name: CYNSN or simply "cellular Yule-Nielsen").

Due to the printing process, the deposited ink dot surface coverage is generally larger than the nominal surface coverage, yielding a "physical" dot gain responsible for the ink spreading phenomenon [4]. An extension of the YNSN model [5] has therefore been proposed to account for ink spreading (name: IS-YNSN). Ink spreading functions are computed by taking into account the respective physical dot gains of an ink halftone printed in different superposition conditions, i.e. in superposition with the different underlying colorants: alone on paper, in superposition with a second solid ink and in superposition with the second and a third solid ink. This yields, for each ink halftone in each superposition condition, an ink spreading curve mapping nominal to effective surface coverages [5]. For predicting the spectral reflectance of a color halftone, effective surface coverages are obtained from nominal surface coverages by weighting the effective surface coverages deduced from the ink spreading curves according to the area coverages of the underlying colorants.

Both the ink spreading and the cellular subdivision enhancements of the Yule-Nielsen model require additional measurements. For CMY prints, the IS-YNSN model requires at least the spectral reflectance of the 50% ink halftones in each superposition condition (3 ink halftones, each in 4 superposition conditions = 12 halftones) plus the spectral reflectance of the 8 Neugebauer primaries, yielding 20 spectral measurements. In case of the cellular Yule-Nielsen model (CYNSN), a single level subdivision requires $3^3 = 27$ spectral primary measurements and a finer level subdivision obtained with combination of 0%, 25%, 50%, 75% and 100% ink surface coverages requires $5^3 = 125$ measurements of spectral primaries.

In prior work, the cellular Yule-Nielsen model was further improved along the following lines:

a) Optimization of the Neugebauer primary reflectances according to the color halftone patches forming the learning set [4].
b) Octtree like hierarchical subdivision of the surface coverage cube and subcubes until the desired prediction accuracy is reached within each leaf subcube [12].
c) Introducing for each ink a single function relying on single ink halftone ramps mapping nominal to effective surface coverages [4] [13].
d) Optimization of the positions for the non-uniform cellular subdivision of the surface coverage unit cube [13].

In the present contribution, we propose an extension of the cellular Yule-Nielsen model accounting for ink spreading

either by fitting the ink spreading curves with one halftone per ink and per subdomain (name: IS-CYNSN) or by fitting them with a single halftone (name: IS_{single}-CYNSN) per subdomain. For both an inkjet print and a laser print, there is a remarkable improvement of the prediction accuracies offered by the proposed IS-CYNSN and IS_{single}-CYNSN model extensions compared with the stand-alone CYNSN model (Sect. 4). In addition, we show that ink spreading can be characterized by measurements from 3 color sensors instead of full spectral measurements without reducing the prediction accuracies (Sect. 3).

Ink spreading for the Cellular Yule-Nielsen model

The Yule-Nielsen modified Neugebauer spectral model Eq. (1) is used to predict the spectral reflectance $R(\lambda)$ of a color halftone as a weighted sum of Neugebauer primary reflectances $R_i(\lambda)$, where a_i is the area coverage of the i^{th} primary, $R_i(\lambda)$ its reflection spectrum and n the Yule-Nielsen value accounting for the lateral propagation of light (in general, $1<n<100$).

$$R(\lambda)=\left(\sum_i a_i R_i(\lambda)^{1/n}\right)^n \tag{1}$$

Hereinafter, we focus on the spectral reflectance prediction models for three inks. However, the models can be extended to 4 inks [6]. With three inks, we have $2^3 = 8$ primaries corresponding to all combinations of 0% and 100% ink surface coverages. Assuming independently printed cyan, magenta and yellow inks, the area coverages a_i of the primaries white (a_w), cyan (a_c), magenta (a_m), yellow (a_y), red (a_r) (superposition of magenta and yellow), green (a_g) (superposition of cyan and yellow), blue (a_b) (superposition of cyan and magenta) and black (a_k) (superposition of cyan, magenta and yellow) are calculated according to the Demichel's equations [7] expressed by Eqs. (2)

$$\begin{aligned} a_w &= (1-c)(1-m)(1-y) & a_c &= c(1-m)(1-y)\\ a_m &= (1-c)m(1-y) & a_y &= (1-c)(1-m)y\\ a_r &= (1-c)my & a_g &= c(1-m)y\\ a_b &= cm(1-y) & a_k &= cmy \end{aligned} \tag{2}$$

where c, m, y represent respectively the cyan, magenta and yellow ink surface coverages. These 8 area coverages are identical to the 8 coefficients used for tri-linear interpolation between known cube vertex values.

Thanks to the cellular Yule-Nielsen extension of the Neugebauer model [4], we improve the prediction accuracy by dividing the CMY ink surface coverage space into 8 subdomains. As Neugebauer primaries, we not only consider reflectances of printed halftones at 0% and 100% surface coverages, but also printed halftones (called subdomain primaries) at all combinations of 0%, 50% and 100% surface coverages ($2^3 = 27$ combinations). Figure 1 illustrates a subdomain where the cyan, magenta and yellow ink surface coverages vary from 0 to 0.5. For ink surface coverages within that subdomain, we first normalize the subdomain coverages. With c, m, y ink surface coverages of cyan, magenta and yellow between 0 and 0.5, the normalized coverages c', m' and y' are

$$c'=\frac{c}{0.5} \qquad m'=\frac{m}{0.5} \qquad y'=\frac{y}{0.5} \tag{3}$$

The areas of the subdomain primaries are calculated from the normalized coverages c', m' and y' with the coefficients expressed by the Demichel's equations (2). The spectral prediction is carried out by tri-linear interpolation, i.e. by weighting the subdomain primary reflectances with the corresponding areas of subdomain primaries according to the Yule-Nielsen equation (1).

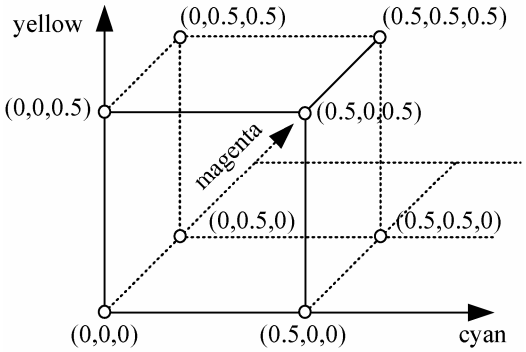

Figure 1. *Illustration of the cellular Yule-Nielsen model where the illustrated cube represents one of the 8 subdomains produced by all combinations of 0%, 50% and 100% surface coverages of the three inks. At the vertices of the cube, subdomain primary reflectances $R_{c,m,y}(\lambda)$ have been measured.*

More precisely, for an arbitrary cellular subdivision and with cyan, magenta and yellow ink surface coverages c, m, y within a subdomain delimited by $c \in [c_l,c_h]$, $m \in [m_l,m_h]$ and $y \in [y_l,y_h]$, the normalized c', m', y' ink coverages are

$$c'=\frac{c-c_l}{c_h-c_l} \qquad m'=\frac{m-m_l}{m_h-m_l} \qquad y'=\frac{y-y_l}{y_h-y_l} \tag{4}$$

The predicted reflectance $R(\lambda)$ of a halftone of surface coverages $c \in [c_l,c_h]$, $m \in [m_l,m_h]$, $y \in [y_l,y_h]$ is obtained by tri-linear interpolation of cube vertex reflectances

$$\begin{aligned} R(\lambda) = \big(&(1-c')(1-m')(1-y')R_{cl,ml,yl}(\lambda)^{1/n}\\ &+c'(1-m')(1-y')R_{ch,ml,yl}(\lambda)^{1/n}+(1-c')m'(1-y')R_{cl,mh,yl}(\lambda)^{1/n}\\ &+(1-c')(1-m')y'R_{cl,ml,yh}(\lambda)^{1/n}+(1-c')m'y'R_{cl,mh,yh}(\lambda)^{1/n}\\ &+c'(1-m')y'R_{ch,ml,yh}(\lambda)^{1/n}+c'm'(1-y')R_{ch.mh,yl}(\lambda)^{1/n}\\ &+c'm'y'R_{ch,mh,yh}(\lambda)^{1/n}\big)^n \end{aligned} \tag{5}$$

where $R_{c,m,y}(\lambda)$ represents the measured spectral reflectance at surface coverages (c,m,y) of the cyan magenta and yellow inks. The prediction accuracy of the cellular Yule-Nielsen model can be improved by a finer subdivision or by multiple levels of subdivisions. For instance, we can increase the number of subdomains by choosing for the subdomain primaries the combinations of 0%, 25%, 50%, 75% and 100% nominal ink surface coverages. In this case, the number of required subdomain primary spectral measurements increases significantly (in the present case: $5^3 = 125$ spectral measurements).

In order to improve the prediction accuracy, as an alternative to the increase of subdomains, we propose an extension of the cellular Yule-Nielsen model where ink spreading is accounted for within each subdomain. We create within each subdomain ink spreading curves expressing the ink spreading behavior of the ink halftone dots. Since the dot gain of one ink within a subdomain does not depend strongly on the other ink surface coverages, we only consider the ink spreading of each ink for a single ink superposition condition. This yields, for each ink i within each subdomain j, an ink spreading curve $f_{i,j}(u'_{i,j})$ mapping the normalized ink coverage $u'_{i,j}$ to a normalized effective ink coverage $u'_{i,j,eff}$. The ink spreading curves are obtained by printing halftones in one ink superposition condition, i.e. with one ink at a nominal surface coverage corresponding to the mid-range of the considered subdomain and the other inks at their lower bounds. For instance, the ink spreading curve for the cyan ink (i=c) within the subdomain j delimited by its low (l) and high (h) bounds $u_{i=c,j} \in [c_{jl}\ c_{jh}]$, $u_{i=m,j} \in [m_{jl},m_{jh}]$ and $u_{i=y,j} \in [y_{jl},y_{jh}]$ is established by printing a halftone at cyan mid-range, magenta low and yellow low bound ink nominal surface coverages, i.e. a halftone at cyan $u_{i=c,j} = (c_{jl} + c_{jh})/2$, at magenta $u_{i=m,j} = m_{jl}$ and at yellow $u_{i=y,j} = y_{jl}$. Then, we fit the mid-range cyan interpolation coefficient $q_{i=c,j}$ of subdomain node reflectances by minimizing the sum of square differences between the measured halftone reflection spectrum ($R_{i=c,j}(\lambda)$) and the corresponding predicted reflectance spectrum ($\hat{R}_{i=c,j}(\lambda)$)

$$
\begin{aligned}
R_{i=c,j}(\lambda) &= R_{(c_{jl}+c_{jh})/2,m_{jl},y_{jl}}(\lambda) \\
\hat{R}_{i=c,j}(\lambda) &= \left(q_{i=c,j}R_{c_{jh},m_{jl},y_{jl}}(\lambda)^{1/n} + (1-q_{i=c,j})R_{c_{jl},m_{jl},y_{jl}}\right)^{1/n} \\
q_{i=c,j} &= \operatorname{argmin}\sum_k\left[R_{i=c,j}(\lambda_k) - \hat{R}_{i=c,j}(\lambda_k)\right]^2
\end{aligned}
\tag{6}
$$

The minimization can be carried out with a computer executable procedure implementing Powell's function minimization [8]. The two other $q_{i=m,j}$ and $q_{i=y,j}$ ink interpolation coefficients of subdomain node reflectances are obtained by replacing the cyan mid-range by the corresponding $u_{i,j}$ mid-range, the cyan higher bound c_{jh} by the $u_{i,j}$ higher bound and keeping in Eq. (6) the other ink coverages at their lower bound. The fitted ink interpolation coefficient $q_{i,j}$ indicates the amount of ink spreading of ink i within the subdomain j. The ink spreading curves $u'_{i,j,eff} = f_{i,j}(u'_{i,j})$ within the subdomain j are obtained by quadratic interpolation between the points (0,0), (0.5,$q_{i,j}$) and (1,1), with $u'_{i,j,eff} = (2 - 4{\cdot}q_{i,j})\ u'^{\,2}_{i,j} + (4{\cdot}\ q_{i,j} - 1)\ u'_{i,j}$.

Computing the interpolation coefficients $q_{i=c,j}$, $q_{i=m,j}$ and $q_{i=y,j}$ with Eq. (6) requires for each subdomain j three spectral reflectance measurements. As an alternative, in order to decrease the number of reflectance measurements to one per subdomain, we propose to jointly fit the interpolation coefficients on a single halftone located at the center of the considered subdomain (Eq. (7))

$$
\begin{aligned}
\hat{R}_{i=center,j}(\lambda) = \Big(& (1-q_{i=c,j})(1-q_{i=m,j})(1-q_{i=y,j})R_{c_{jl},m_{jl},y_{jl}}(\lambda)^{1/n} \\
& + q_{i=c,j}(1-q_{i=m,j})(1-q_{i=y,j})R_{c_{jh},m_{jl},y_{jl}}(\lambda)^{1/n} \\
& + (1-q_{i=c,j})q_{i=m,j}(1-q_{i=y,j})R_{c_{jl},m_{jh},y_{jl}}(\lambda)^{1/n} \\
& + (1-q_{i=c,j})(1-q_{i=m,j})q_{i=y,j}R_{c_{jl},m_{jl},y_{jh}}(\lambda)^{1/n} \\
& + (1-q_{i=c,j})q_{i=m,j}q_{i=y,j}R_{c_{jl},m_{jh},y_{jh}}(\lambda)^{1/n} \\
& + q_{i=c,j}(1-q_{i=m,j})q_{i=y,j}R_{c_{jh},m_{jl},y_{jh}}(\lambda)^{1/n} \\
& + q_{i=c,j}q_{i=m,j}(1-q_{i=y,j})R_{c_{jh},m_{jh},y_{jl}}(\lambda)^{1/n} \\
& + q_{i=c,j}q_{i=m,j}q_{i=y,j}R_{c_{jh},m_{jh},y_{jh}}(\lambda)^{1/n}\Big)^n \\
\left\{q_{i=c,j},q_{i=m,j},q_{i=y,j}\right\} = \operatorname{argmin}\sum_k & \left[R_{i=center,j}(\lambda_k) - \hat{R}_{i=center,j}(\lambda_k)\right]^2
\end{aligned}
\tag{7}
$$

Figure 2 illustrates a cyan dot gain curve for a *cmy* laser print, where the normalized dot gain is defined as $d_{i,j}(u'_{i,j}) = f_{i,j}(u'_{i,j}) - u'_{i,j}$, within the subdomain j=1 delimited by $c \in [0,0.5]$, $m \in [0,0.5]$ and $y \in [0,0.5]$. The computed cyan interpolation coefficient $q_{i=c,1}$ of subdomain node reflectances for an optimal n-value = 14 calculated with Eq. (6) is equal to 0.61. It represents a normalized dot gain of 0.11 in the range [0,1] and therefore a real dot gain of 0.055 in the range [0,0.5]. The cellular Yule-Nielsen model prediction error for the considered halftone without taking into account the dot gain is ΔE_{94} = 3.60. Introducing the dot gain obtained by the fitted cyan interpolation coefficient $q_{i=c,j}$ of subdomain node reflectances decreases for this halftone the prediction error to ΔE_{94} = 0.22. Since for the present print configuration, the ink dot gain within each subdomain j is at least 0.1, accounting for ink spreading considerably increases the spectral prediction accuracy.

When computing the interpolation coefficients $q_{i,j}$ of all subdomains j according to Eq. (7) instead of Eq. (6), the coefficients are similar, i.e. the dot gains do not deviate by more than 10%. We therefore obtain the same prediction accuracy improvements by jointly fitting the interpolation coefficients on a single center subdomain halftone reflectance as when fitting them on the three spectral reflectance measurements required by Eq. (6).

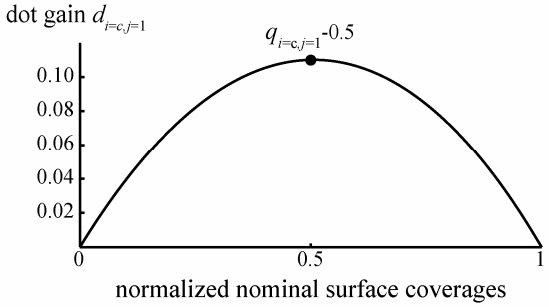

Figure 2. *Cyan dot gain curve corresponding to the cyan ink spreading curve within the subdomain c,m,y ∈ [0,0.5], for a cmy laser print (Brother 4000-HL) at a screen frequency of 120lpi and using an optimal n-value of 14.*

Note that the optimal n-value is found by predicting for successive n-values with the full model all mid-range reflectances. The n-value yielding the minimal average prediction error is kept as the optimal n-value for the considered setup of printer, inks and paper.

The cellular Yule-Nielsen model accounting for ink spreading (IS-CYNSN and IS_{single}-CYNSN) is illustrated in Figure 3. At model calibration, the subdomain ink spreading curves $f_{i,j}(u'_{i,j})$ are established either by separately fitting the interpolation coefficients with Eq. (6) (IS-CYNSN) or by jointly fitting the interpolation coefficients with Eq. (7) (IS_{single}-CYNSN). At run time, nominal ink surface coverages of the considered halftone are normalized according to Eq. (4), the normalized effective ink surface coverages are deduced by making use of the corresponding ink spreading curves, the normalized effective areas of the subdomain primary reflectances are calculated according to Eq. (2) and the halftone reflection spectrum is predicted according to Eq. (1).

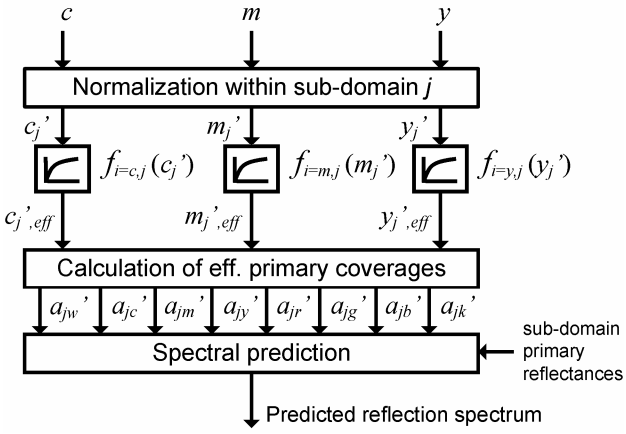

Figure 3. *Cellular Yule-Nielsen model accounting for ink spreading.*

Characterizing ink spreading with sensor responses

The non-cellular ink spreading Yule-Nielsen modified spectral Neugebauer model (IS-YNSN) is calibrated with 8 Neugebauer primaries [5]. In addition, in order to account for ink spreading in all ink superposition conditions, 12 ink spreading curves are established mapping nominal surface coverages to effective surface coverages. In this setup, the model requires 8 + 12 = 20 spectral measurements. In the case of the ink spreading cellular Yule-Nielsen models, one level of subdivision requires 27 subdomain primaries. Ink spreading is modeled by establishing 3 ink spreading curves within each of the 8 subdomains (Sect. 2). Thus, in case of separately fitted coefficients, the IS-CYNSN model requires 27 +8·3 = 51 measurements and in case of jointly fitted the interpolation coefficients, the IS_{single}-CYNSN model requires 27+8·1 = 35 measurements.

However, since establishing the ink spreading curves requires fitting only one scalar variable (IS-CYNSN) or three scalars (IS_{single}-CYNSN) at a time, it is possible to use for example red, green and blue sensor responses for the fitting process [9]. The ink spreading characterization of the IS-YNSN, the IS-CYNSN and the IS_{single}-CYNSN is performed by minimizing the sum of square differences between predicted and measured sensor response values. Fitting with sensors considerably reduces the number of required spectral measurements. Only the spectral measurements of Neugebauer primaries are necessary, 8 for the IS-CYNSN model and 27 for a single level subdivision IS-CYNSN and IS_{single}-CYNSN models. In order to demonstrate the feasibility of using sensor responses instead of spectral measurements, we simulate the RGB sensor devices by the DIN-16536-2 standard RGB sensitivities for densitometric measurements [10]. Samples are illuminated with a standard CIE D65 illuminant. Reflected light generates the sensor responses C_i

$$C_i = \sum_k S_i(\lambda_k)R(\lambda_k)I(\lambda_k) \Big/ \big(I(\lambda_k)S(\lambda_k)\big) \tag{8}$$

where C_i represents the i^{th} sensor response value, S_i the spectral sensitivity of the i^{th} sensor, $I(\lambda)$ the illuminant and $R(\lambda)$ the spectral reflectance [11]. We can fit the interpolation coefficients $q_{i,j}$ of subdomain node reflectances by replacing in Eq. (6), respectively in Eq. (7) predicted and measured reflectances by their corresponding $C_{i,j}$ and $\hat{C}_{i,j}$ sensor responses, according to Eq (8).

Let us consider as example the *cmy* laser print. The three dot gain curves within the subdomain shown in Figure 1 are similar one to another. The interpolation coefficients $q_{i=c,j=1}$, $q_{i=m,j=1}$ and $q_{i=y,j=1}$ of nodes reflectances are either respectively equal to 0.6050, 0.5989 and 0.5912 when fitted with the spectral reflectance metric or respectively equal to 0.6069, 0.6000 and 0.5945 when fitted with the simulated RGB sensor response metric. The interpolation coefficients of subdomain node reflectances $q_{i,j}$ in all subdomains j do not deviate by more than 1.5% when comparing these two metrics. Therefore, the prediction accuracy remains the same when characterizing ink spreading for the IS-CYNSN, the IS-YNSN and the IS_{single}-CYNSN models with three sensor responses instead of spectral measurements.

Results

We performed spectral predictions with the cellular Yule-Nielsen model, the ink spreading enhanced cellular Yule-Nielsen models and the ink spreading enhanced Yule-Nielsen model (Table 1). In order to compare the resulting prediction accuracies with prior work, we also consider for each ink a single global ink spreading function, which is fitted with the YNSN model at 25%, 50%, 75% nominal ink surface coverages. We also performed spectral predictions by characterizing ink spreading with simulated RGB sensors for both the IS-CYNSN and the IS-YNSN models (Table 2). The experiments were performed on an ink jet printer (Canon Pixma Pro 9500 at 600 dpi) with standard cyan, magenta and yellow inks printed on Canon MP-101 paper at a screen frequency of 120lpi. In addition, test samples were printed with a laser printer (Brother 4000-HL at 600 dpi) with standard cyan, magenta and yellow toners on Canon MP-101 paper at a screen frequency of 120 lpi. The tests samples were printed at all combinations of nominal ink surface coverages 0, 0.25, 0.5, 0.75 and 1 (5^3 = 125 test patches) with a classical rotated

screen. Reflectances were measured with a GretagMacBeth Color i7 spectrophotometer with geometry (d:8^0) under a D65 illuminant. Table 1 and Table 2 give the mean prediction error in terms of ΔE_{94} values, the maximal prediction error, the 95% quantile prediction error, the average rms reflectance prediction error, the number of spectral primary reflectance measurements (p) and the number of ink spreading measurements (i). The n-value yielding the best prediction accuracies for all models and test sets is 14.

The spectral prediction based on the proposed ink spreading extension for the cellular Yule-Nielsen model (IS-CYNSN) provides a significantly higher prediction accuracy compared with the stand-alone cellular Yule-Nielsen model (CYNSN). The ΔE_{94} mean prediction error decreases from 2.29 to 1.06 for a laser print (Table 1, Brother 4000-HL test set) and from 0.92 to 0.54 for a classical CMY ink jet print (Table 1, Canon pro 9500 test set). When printing with a laser printer (Brother 4000-HL), we observe a strong dot gain within all surface coverage subdomains. Therefore, for this printer, there is a large difference in prediction accuracy between the IS-CYNSN model that accounts for ink spreading and the CYNSN model that does not account for ink spreading. In addition, considering ink spreading within each subdomain also offers a higher prediction accuracy than when using within the CYNSN model for each ink a single global function mapping nominal to effective surface coverages (IS_{global}-CYNSN), i.e. the ΔE_{94} mean prediction error decreases from 1.30 to 1.06 for the laser print and from 0.70 to 0.54 for the ink-jet print.

Introducing ink spreading within each subdomain by jointly fitting the interpolation coefficients provides higher prediction accuracies than by separately fitting the interpolation coefficients. For instance, in case of the Canon pro 9500 print, with the IS-CYNSN model, we obtain a ΔE_{94} mean prediction error of 0.54 and a 95% quantile prediction error of 1.49 and with the IS_{single}-CYNSN these prediction errors decrease respectively to 0.38 and to 0.99. This can be explained by the fact that the center of each subdomain contains the most useful information in respect to the ink spreading phenomenon. The IS_{single}-CYNSN represents therefore an excellent tradeoff between number of measurements and prediction accuracy. With only 35 spectral reflectance measurements we obtain remarkable predictions accuracies. Similar tests have been conducted on an offset print, a proofing device (Kodak Approval) and other ink-jet prints. In all cases, mean prediction ΔE_{94} errors around 0.4 have been obtained.

We also remarked that the ink spreading enhanced Yule-Nielsen model that accounts for ink spreading without cellular subdivision is more accurate than the cellular Yule-Nielsen model. This can be explained by the fact that the ink spreading behavior of multi-ink halftones is well captured by the Yule-Nielsen spectral Neugebauer model enhanced to account for ink spreading in all superposition conditions.

The spectral prediction accuracies obtained when characterizing ink spreading with RGB sensors for the IS-CYNSN, the IS_{single}-CYNSN, the IS_{global}-CYNSN and the IS-YNSN models (Table 2) are nearly identical with the ones obtained with ink spreading characterized by spectral measurements (Table 1). This shows that the ink spreading characterization can be performed by making use of RGB sensors instead of using spectral reflectance measurements. The cost of including RGB sensors within printers is much lower compared with the cost of including a spectrophotometer. Therefore, the ink spreading enhancement of the non-cellular as well as the cellular Yule-Nielsen models offers the potential of characterizing printers at run time at a moderate cost.

Table 1. Prediction accuracies for cyan, magenta, yellow test samples printed with a Canon pro 9500 ink jet printer and for cyan, magenta and yellow test samples printed with a Brother 4000-HL laser printer.

Test sets	# measurements	ΔE_{94}			*rms*
Model	*p+i*	avg	95%	max	avg
Brother 4000-HL					
Prior art:					
CYNSN	27+0 = 27	2.29	5.22	6.53	0.02009
IS_{global}-CYNSN	27+9 = 36	1.30	3.31	3.79	0.01072
IS-YNSN	8+12 = 20	1.86	4.10	5.01	0.01544
New:					
IS-CYNSN	27+24 = 51	1.06	3.06	3.76	0.00695
IS_{single}-CYNSN	27+8 = 35	0.96	2.62	3.23	0.00741
Canon pro 9500					
Prior art:					
CYNSN	27+0 = 27	0.92	2.15	3.03	0.00549
IS_{global}-CYNSN	27+9 = 36	0.70	1.86	2.30	0.00408
IS-YNSN	8+12 = 20	0.85	1.94	2.17	0.00665
New:					
IS-CYNSN	27+24 = 51	0.54	1.49	2.08	0.00327
IS_{single}-CYNSN	27+8 = 35	0.38	0.99	1.40	0.00274

Table 2. Prediction accuracies for both the IS-YNSN model and the IS-CYNSN models when characterizing the ink spreading using simulated RGB sensors.

Test sets	# measurements	ΔE_{94}			*rms*
Model	*p+i*	avg	95%	max	avg
Brother 4000-HL					
IS_{global}-YNSN	27+9 = 36	1.31	3.28	3.77	0.01080
IS-YNSN	8+12 = 20	1.88	4.09	4.93	0.01502
IS-CYNSN	27+24 = 51	1.15	3.29	3.94	0.00732
IS_{single}-CYNSN	27+8 = 35	0.99	2.74	3.23	0.00749
Canon pro CMY					
IS_{global}-YNSN	27+9 = 36	0.70	1.92	2.36	0.00419
IS-YNSN	8+12 = 20	0.74	1.71	2.00	0.00575
IS-CYNSN	27+24 = 51	0.57	1.59	2.14	0.00367
IS_{single}-CYNSN	27+8 = 35	0.38	1.05	1.47	0.00289

Conclusion

We propose an extension of the cellular Yule-Nielsen spectral Neugebauer model by accounting for ink spreading separately within each subdomain. The ink spreading characterization of the cellular Yule-Nielsen model can be established by jointly fitting the ink spreading interpolation coefficients on a single halftone centered within each of the subdomains. We obtain excellent spectral prediction accuracies with only a small number of measurements. Compared with the original cellular Yule-Nielsen model, prediction accuracies are significantly improved. In addition, the ink spreading characterization can be performed with RGB sensors without

reduction of prediction accuracy. This offers the potential of characterizing printers at run time at a moderate cost.

Acknowledgement

We thank the Swiss National Science Foundation for its support, grant n° 200020-126757/1.

References

[1] J.A.C. Yule, W.J. Nielsen, The penetration of light into paper and its effect on halftone reproductions, Proc. TAGA, Vol. 3, 65-76, 1951.

[2] J.A.S Viggiano, Modeling the Color of Multi-Colored Halftones, Proc. TAGA, 44-62, 1990.

[3] K. J. Heuberger, Z. M. Jing, and S. Persiev, Color Transformations and lookup tables, in Proc. 1992 TAGA/ISCC, pp. 863-881.

[4] R. Balasubramanian, Optimization of the spectral Neugebauer model for printer characterization, J. Electronic Imaging, Vol. 8, No. 2, 156-166, 1999.

[5] R.D. Hersch, F. Crété, Improving the Yule-Nielsen modified spectral Neugebauer model by dot surface coverages depending on the ink superposition conditions, Color Imaging X: Processing, Hardcopy and Applications, SPIE Vol. 5667 (R. Eschbach, G.G. Marcu eds.), 434-445, 2005.

[6] T. Bugnon, M. Brichon, R.D. Hersch, Simplified Ink Spreading Equations for CMYK Halftone Prints, Proc. SPIE Vol. 6807, paper 680717-1 to 12, 2008.

[7] David R. Wyble, Roy S. Berns, A critical review of spectral models applied to binary color printing, Color research and application, Vol. 25, No.1, 4-19, 2000.

[8] W.H. Press, B.P. Flannery, S.A. Teukolsky, W.T. Fetterling, Numerical Recipes, Cambridge University Press, 1st edition, 1988, section 10.5, pp. 309-317.

[9] N. P. Garg, A. K. Singla and R.D. Hersch, Calibrating the Yule-Nielsen Modified Spectral Neugebauer Model with Ink Spreading Curves Derived from Digitized RGB Calibration Patch Images, J. Imaging Sci. Technol., Vol. 52, No. 4, paper 40908, 5 pages, 2008.

[10] Din Deutches Institut für Normung e.V., Prüfung von Drucken und Druckfarben der Druckteknik, Teil 2: Anforderungen an die Messanordnung von Farbdichtemessgeräten und ihre Prüfung, Ref. Nr. DIN 16536-2, 1995.

[11] Raja Bala, Device characterization (Chapter 5), Sect. 5.2.3, Input device calibration and characterization in Digital Color Imaging Handbook, Ed. G. Sharma, CRC Press, 275-281, 2003.

[12] U. Agar, J. P. Allebach, An iterative cellular YNSN method for color printer characterization, Proc. 6th Color imaging conf., IS&T, 197-200, 1998.

[13] Y. Chen, Roy S. Berns and L. A. Taplin, Six Color Printer Characterization Using an Optimized Cellular Yule-Nielsen Spectral Neugebauer Model, J. Imaging Sci. Technol., Vol. 48, No. 6, 519-528, 2004.

Author Biography

Romain Rossier *is a PhD student at the Peripheral Systems Laboratory (Ecole Polytechnique Fédérale de Lausanne, or EPFL) in Lausanne, Switzerland. His research interests include color prediction, mathematical modeling of printing processes, color printing with ink jet and security imaging. He obtained his master degree in computer science from EPFL in 2007.*

